NORGES TEKNISK-NATURVITENSKAPELIGE
UNIVERSITET

Adaptive spectral methods

by

Øystein Tråsdahl[1] and Einar M. Rønquist[1]

PREPRINT
NUMERICS NO. 1/2012

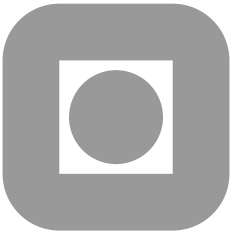

NORWEGIAN UNIVERSITY OF
SCIENCE AND TECHNOLOGY
TRONDHEIM, NORWAY

This report has URL
http://www.math.ntnu.no/preprint/numerics/2012/N1-2012.pdf
Address: Department of Mathematical Sciences, Norwegian University of Science and Technology, N-7491 Trondheim, Norway.

[1]Email: {trasdahl,ronquist}@math.ntnu.no

Adaptive spectral methods

Øystein Tråsdahl[†] and Einar M. Rønquist[†]

January 31, 2012

This paper discusses numerical solution of boundary value problems using spectral methods combined with nonlinear and adaptive mappings between the reference domain and the physical domain. A brief review of existing methods for adaptive mesh generation is given, and a method for finding close to optimal mappings for boundary value problems in $\mathbb{R}^1$ is presented. The method exploits the link between high order numerical solutions of PDEs and approximation of parametric curves. Also, other adaptive methods for boundary value problems in $\mathbb{R}^1$ are proposed, based either on minimizing the discrete L^2-norm of the residual, or interpolating the residual as a parametric curve. The adaptive methods are constructed with the aim of finding optimal mappings, however, this turns out to be a very difficult task. Still, significant improvement from standard (non-adaptive) high order methods is achieved in some cases.

Keywords: Spectral methods, optimal mesh, advection-diffusion equation

1 Introduction

Spectral and pseudo-spectral (PS) methods are attractive methods for the numerical solution of partial differential equations (PDEs) for which the solution, the geometry and the source terms have a high degree of regularity. In particular, for analytic solution and data, the error in the numerical solution decreases exponentially fast as the dimension of the approximation space increases [6, 10]. This convergence rate is related to the global approach of the spectral and PS methods: the basis functions (trigonometric or algebraic polynomials) have global support, and the convergence rate is inherited from the convergence rate of classical trigonometric or polynomial approximation. Compared with finite difference and finite element methods, which are based on local approximations of fixed (low) order, this can lead to significantly smaller errors for a given number of degrees-of-freedom.

However, there are problems where spectral and PS methods are considered less suitable. If the solution has a boundary or interior layer with steep gradients, then small errors will only be achieved when the polynomial degree is high enough to resolve the localized phenomena. One such class of problems is singularly perturbed boundary value problems. For example, considering the advection-diffusion equation, a high Peclet number may yield a solution with a thin boundary layer, and the numerical solution may be corrupted by oscillations, spreading globally over the computational domain (unless the resolution is high enough). The thinner the boundary layer is, the larger the oscillations are for a

[†]Email: {trasdahl,ronquist}@math.ntnu.no

fixed resolution (or polynomial degree). These problems are common for most numerical methods, including finite difference and finite element methods. However, these are cheaper and easier to refine locally to the required resolution [2, 26]. For this reason, adaptivity is much more developed in the context of low order methods than for spectral methods.

There have been a number of strategies proposed for overcoming these difficulties in the context of spectral and PS methods. One option is post-processing the solution through filtering, which can be used to dampen oscillations. This requires a modal representation of the numerical solution. Another option is the addition of artificial viscosity. Tadmor introduced the vanishing viscosity method for shock capturing [22, 23]. Brezzi et. al. [8] introduced bubble stabilization in a finite element context, in which the space of test functions is augmented by a set of "bubble functions". The ideas were applied to spectral methods by Canuto [9] and Pasquarelli and Quarteroni [20].

Adaptive methods can also be based on modifying the mesh on which the spectral solution is represented. A spectral Galerkin approach typically involves applying a coordinate transformation, solving the PDE in a *reference domain* using a standard mesh, and then mapping the numerical (polynomial) solution back to the *physical domain* to approximate the exact solution. A key idea with adaptive methods is that, to achieve sufficient resolution in the interior or boundary layers, mesh nodes are clustered in these critical regions in the physical domain. For low order methods this always leads to a better approximation, but for high order methods based on polynomials, the issue is a bit more complicated. A high mesh node density may not necessarily mean better accuracy, since the numerical solution may display wild oscillations *between* the nodes. The method may not even converge as the number of nodes increases. The key to constructing good adaptive meshes in the context of high order methods is regularity: the reference domain must be mapped to the physical domain by a *smooth coordinate transformation* in order to avoid oscillations. Enforcing a smooth and yet suitably adaptive mapping is difficult, and few authors address the regularity of the mapping explicitly. The adaptive methods are often based on some other requirement, for example equidistribution of some function over the computational domain, or minimization of some norm of the numerical solution. An overview over existing adaptive methods in this category is given in Section 3.

The objectives of this paper are to investigate optimal or close to optimal mappings for the numerical solution of boundary value problems and to test adaptive methods that are constructed with the aim of finding such mappings. The paper is structured as follows: in Section 2 the potential of adaptive methods is demonstrated through the numerical solution of a one-dimensional advection-diffusion model problem, and the role of the coordinate transformation is briefly discussed. We then proceed in Section 3 with a review of existing adaptive methods in the high order context. In Sections 4 and 5 we present methods for constructing close to optimal and approximate coordinate transformations, respectively; these methods are based on interpolation of parametric curves, and the link between interpolation and adaptive high order methods is explained. In Sections 6 and 7 we introduce alternative adaptive methods, and in Section 8 some additional numerical results are presented. Finally, in Section 9, we present some conclusions and remarks.

2 A motivational example

To show the potential of adaptivity in the context of spectral methods, we begin with an example. The problems we will consider in this paper are advection-diffusion boundary

value problems that can be written on the form

$$-\varepsilon \frac{\mathrm{d}^2 u}{\mathrm{d}x^2} + \frac{\mathrm{d}u}{\mathrm{d}x} = f, \qquad x \in \Omega, \tag{1}$$

accompanied by suitable boundary conditions. Here, ε is a constant, f is a smooth function, and Ω is a bounded interval on the real axis.

Consider a particular model problem on the form (1) where $\Omega = (0,1)$, $\varepsilon = 0.01$, $f(x) = 1$, and with homogeneous Dirichlet boundary conditions. The problem has the exact solution

$$u(x) = x - \frac{e^{x/\varepsilon} - 1}{e^{1/\varepsilon} - 1}, \tag{2}$$

which features a boundary layer with a width of order $\mathcal{O}(\varepsilon)$ near $x = 1$.

A pure spectral method is applied to solve the problem numerically. It is based on the equivalent weak form of (1), and can be stated as follows: find $u \in X = H_0^1(\Omega)$ such that

$$a(u, v) = (f, v), \qquad \forall v \in X, \tag{3}$$

where

$$a(u, v) = \varepsilon \int_\Omega \frac{\mathrm{d}u}{\mathrm{d}x} \frac{\mathrm{d}v}{\mathrm{d}x} \, \mathrm{d}x + \int_\Omega \frac{\mathrm{d}u}{\mathrm{d}x} v \, \mathrm{d}x, \tag{4}$$

and

$$(f, v) = \int_\Omega f v \, \mathrm{d}x. \tag{5}$$

Prior to discretization both integrals are transformed to integrals over a reference domain $\widehat{\Omega} = (-1, 1)$. The coordinate transformation is given by $x = \mathcal{F}(\xi)$, with $x \in \Omega$, $\xi \in \widehat{\Omega}$. Discretization is based on high order polynomials over $\widehat{\Omega}$, and the discrete space $X_N \subset X$ can be expressed as

$$X_N = \{v \in X, v \circ \mathcal{F} \in \mathbb{P}_N(\widehat{\Omega})\}. \tag{6}$$

Exact integration of the bilinear and linear forms is replaced by quadrature at the Gauss-Lobatto Legendre (GLL) points. The numerical solution $\hat{u}_N = u_N \circ \mathcal{F}$ is a polynomial of degree N over $\widehat{\Omega}$, and it can be represented by the nodal basis

$$\hat{u}_N(\xi) = \sum_{j=0}^{N} u_j \ell_j(\xi). \tag{7}$$

Here, ℓ_j is a Lagrangian interpolant through the GLL points $\xi_0, \ldots, \xi_N$, i.e., it is the unique polynomial of degree N satisfying $\ell_j(\xi_k) = \delta_{jk}$. The functions $\ell_0, \ldots, \ell_N$ make up a basis for the space $\mathbb{P}_N(\widehat{\Omega})$ of polynomials of degree less than or equal to N over $\widehat{\Omega}$. Note that in (7) the basis coefficients $u_0 = u_N = 0$ due to the homogeneous boundary conditions, and $u_j = \hat{u}_N(\xi_j) = u_N(x_j)$, with $x_j = \mathcal{F}(\xi_j)$.

The difference between the exact solution and the numerical solution measured in the L^2 norm is given by

$$||u - u_N||^2_{L^2(\Omega)} = \int_\Omega \Big(u(x) - u_N(x)\Big)^2 \, \mathrm{d}x. \tag{8}$$

Again, the integral can be transformed to an integral over $\widehat{\Omega}$ and exact integration can be replaced by GLL quadrature. In practice, overintegration in $M \gg N$ quadrature points is used in order to ensure that the quadrature error is subdominant the discretization error.

Solving the boundary value problem over a reference domain requires a bijective mapping between $\widehat{\Omega}$ and Ω. Of course, the easiest, and certainly the most common, option is to use a linear (or affine) mapping, $\mathcal{F} = \overline{\mathcal{F}}$, given explicitly as

$$x = \overline{\mathcal{F}}(\xi) = \frac{\xi + 1}{2}. \tag{9}$$

However, we may also consider more general (nonaffine) mappings $\mathcal{F} : \widehat{\Omega} \to \Omega$. There is nothing in the spectral method that requires $\mathcal{F}$ to be linear; the only requirement is that it is bijective. Note that the numerical solution is not constructed as a polynomial approximation of u, but rather of the mapped solution

$$u(\mathcal{F}(\xi)) = (u \circ \mathcal{F})(\xi) = \hat{u}(\xi). \tag{10}$$

The standard error estimates apply to $\hat{u}$, so using $\mathcal{F}$ to increase the smoothness of $\hat{u}$ may increase the convergence rate.

A consequence of using a nonlinear mapping is that the test functions are no longer polynomials when viewed as functions on the physical domain. This is discussed in [21], where optimal error estimates are derived.

Let us now solve the model problem using a polynomial degree $N = 10$ and two different mappings $\mathcal{F}$: the affine mapping (9), and a customized, nonlinear mapping determined by the ET method described in Section 4. Figure 1 shows the two numerical solutions over both the physical domain and the reference domain. The affine mapping results in an oscillatory numerical solution due to the failure of resolving the boundary layer. On the other hand, the nonlinear $\mathcal{F}$ gives a numerical solution that cannot be distinguished from the exact solution. Figure 2 shows that this mapping is highly nonlinear, and that it moves all the GLL points in the direction of the boundary layer.

3 A review of adaptive high order methods

Adaptive mesh generation in the context of spectral and pseudo-spectral (PS) methods has been investigated for several decades. Although some progress has been made, a lot remains to be done in order for this to represent a practical and efficient tool. This is in contrast to adaptive low order methods (e.g., hp-FEM), which is a mature field and also widely used in commercial applications. The reason for the relative lack of breakthrough is probably the complexity and the cost associated with constructing a global mapping which will minimize the discretization error for a fixed order of approximation.

In the literature, adaptivity for high order methods is most often applied to problems with interior or boundary layers. This is the area where such methods have the biggest potential and where the effect of adaptivity is the most striking. Standard high order methods may yield exponential convergence for such problems, but small error levels are typically achieved only after the interior or boundary layer has been properly resolved, and then often at a very low (exponential) rate [27]. An adaptive mapping will typically cluster (physical) grid points in the region(s) in Ω where the exact solution u changes rapidly, effectively "stretching out" the corresponding region in $\widehat{\Omega}$, yielding slower variation and less step gradients in the mapped solution $\hat{u}$.

Most adaptive methods can be applied to time-independent problems, but they are more often applied to time-dependent problems. This is because such problems lend themselves well to most of the existing adaptive algorithms. The numerical solution from the current time step contains valuable information about the variation that will occur in the solution

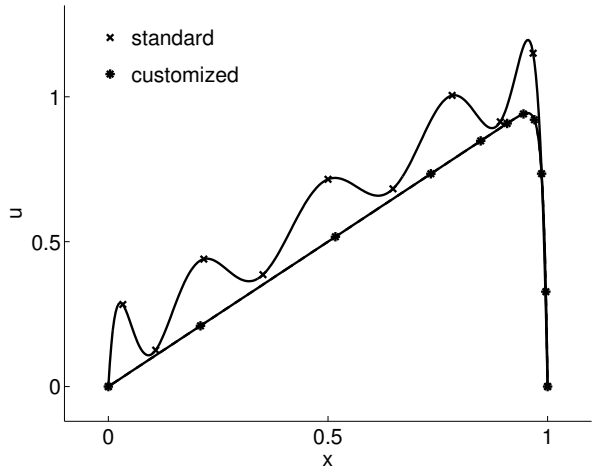

(a) Exact and numerical solutions in Ω

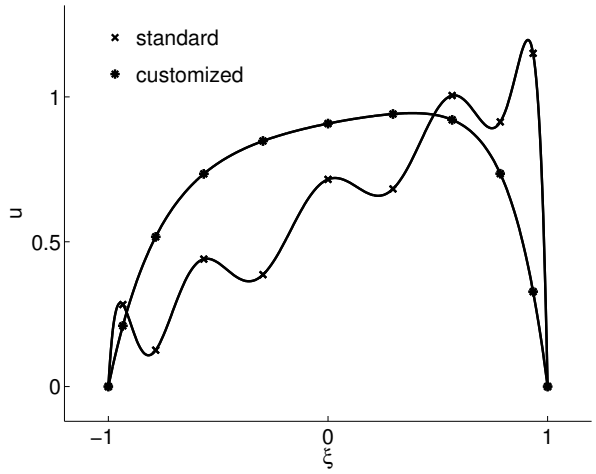

(b) Numerical solutions in $\widehat{\Omega}$

Figure 1: Two numerical solutions of an advection-diffusion problem with exact solution (2), solved using a pure Legendre spectral method. Using an affine mapping $\mathcal{F}$ (`standard`) from the reference domain $\widehat{\Omega}$ to the physical domain Ω gives poor resolution of the boundary layer near $x = 1$ and therefore unwanted oscillations in the numerical solution u_N. Using a customized, nonlinear $\mathcal{F}$ (`customized`) smooths out the variation in $\hat{u}$ over $\widehat{\Omega}$ and gives sufficient resolution of the localized effects, resulting in a vastly better numerical solution.

at the next time step. In time-independent problems, adaptivity either involves an *a priori* asymptotic analysis to disclose the position (and width) of interior and boundary layers, or an iterative method is employed to gradually discover these features.

The analysis of adaptive spectral and PS methods can essentially be done in two ways: on the reference domain or on the physical domain. With the former approach, the basis functions are not mapped and standard tools can be applied. The difficulty lies in the PDE, which must be mapped from the physical domain by the inverse of $\mathcal{F}(\xi)$ and can be very complex. The latter approach allows us to consider the original PDE, but now the basis functions are mapped, and specialized tools must be developed. Wang and Shen used this approach when they derived optimal error estimates for mapped Legendre spectral methods in [21] and for mapped Jacobi spectral methods in [27].

The simplest adaptive mesh generation methods are not really adaptive, in that they

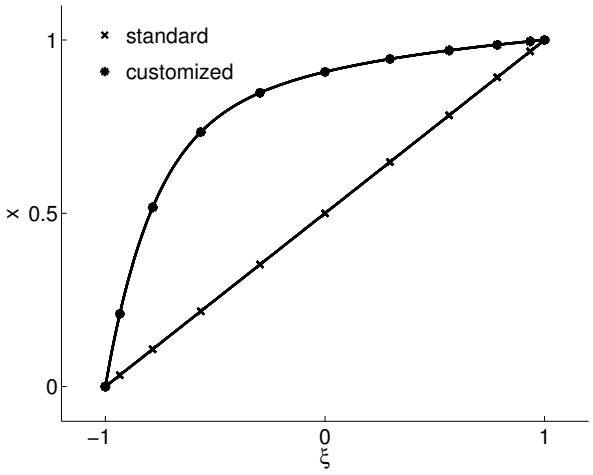

Figure 2: The two mappings $x = \mathcal{F}(\xi)$ used to produce the two numerical solutions shown in Figure 1. The affine (`standard`) mapping corresponds to the oscillatory solution, and the nonlinear (`customized`) mapping corresponds to the solution that cannot be distinguished from the exact solution.

simply *choose* the structure of $\mathcal{F}$ without using any information about the exact solution. In [17] the mapping

$$\mathcal{F}(\xi;\lambda) = -1 + \sigma_\lambda \int_{-1}^{y} (1-t^2)^\lambda \, \mathrm{d}t \tag{11}$$

is used, where σ_λ is a constant depending on λ, and λ is a parameter to be determined. For $-1 < \lambda < 0$ the mesh nodes are moved towards the origin, and for $\lambda > 0$ they are clustered near the end points. The authors choose $\lambda = 1$ in their numerical experiments and solve various boundary value problems with a modified Legendre spectral method. They also extend their method to two-dimensional problems.

Similarly, in [24] Tang and Trummer use a transformation $\mathcal{F}_m(\xi)$ consisting of iterated sine functions, defined recursively by

$$\mathcal{F}_m(\xi) = \sin(\frac{\pi}{2}\mathcal{F}_{m-1}(\xi)), \qquad \mathcal{F}_0(\xi) = \xi. \tag{12}$$

As m increases, the mesh nodes are clustered more densely at the end points of the physical interval. The authors test their mappings on one-dimensional boundary value problems for different $m \leq 3$.

A common approach in adaptive high order methods is to restrict $\mathcal{F}$ to be a function on a particular, *a priori* chosen form, with one or more free parameters. Adaptivity is then simplified to the task of determining suitable values for these parameters. This is the approach adopted by Kosloff and Tal-Ezer [16], who use a mapping

$$\mathcal{F}(\xi;\lambda) = \frac{\arcsin(\lambda\xi)}{\arcsin(\lambda)}, \qquad 0 < \lambda < 1, \tag{13}$$

which stretches a Gauss-Lobatto Chebyshev (GLC) grid toward a uniform grid as $\lambda \to 1^-$. They discuss various considerations for choosing the parameter λ: enabling resolution of the largest possible wave number, or optimizing for interpolation of a general trigonometric function. An adaptive approach is to choose the parameters such that the function to be approximated can be represented by a Chebyshev expansion with the minimal number of terms. The authors show that a suitable choice leads to a differentiation matrix D

whose eigenvalues are all $\mathcal{O}(N)$, where N is the polynomial degree, reducing the time step restriction in explicit time integration methods.

In the adaptive methods proposed in [1, 4, 5] the parameters in $\mathcal{F}$ are chosen so that the numerical solution minimizes some chosen functional. The mappings used are two-parameter functions composed of trigonometric and inverse trigonometric functions, e.g.,

$$\mathcal{F}(\xi;\lambda_1,\lambda_2) = 1 + \frac{4}{\pi}\arctan(\lambda_1 \tan(\frac{4}{\pi}(\frac{\lambda_2 - x}{\lambda_2 x - 1} - 1))), \quad \lambda_1 > 0, \quad -1 < \lambda_2 < 1, \tag{14}$$

where λ_1 relates to the width and λ_2 to the position of an interior or boundary layer in the exact solution. The functional to be minimized is typically a measure of the total variation in the solution, for example the Sobolev norm

$$\mathcal{J} = \int_\Omega (u^2 + u_x^2 + u_{xx}^2)\, \mathrm{d}x. \tag{15}$$

The idea is that minimizing $\mathcal{J}$ means reducing unwanted oscillations, since these can give large contributions to $\mathcal{J}$ through the second derivative of u. A good mapping yields a solution with few (or no) unwanted oscillations, and hence a low value of $\mathcal{J}$. The interpolation and integration in the minimization procedure introduces some significant overhead, but on the other hand, vast improvements in convergence rate may be achieved.

Tee and Trefethen [25] choose a particular two-parameter mapping $\mathcal{F}$ based on how it maps singularities of the exact solution in the complex plane. The parameters are chosen to enlarge the *ellipse of analyticity* of $\hat{u}$, which is the largest ellipse with foci ± 1 in which $\hat{u}$ has no singularities. This immediately increases the convergence rate of the rational spectral collocation method, since the error is of order $\mathcal{O}((L+l)^{-N})$, where L and l are the semi-axes of the ellipse [3]. The method in [25] is limited to cases where u has one pair of complex conjugated singularities, but it is extended to problems with multiple pairs of singularities in [14].

Another family of adaptive mesh methods are based on equidistribution of some monitor or weight function over the physical domain. Such methods must consider general $\mathcal{F}$, since it is not given that equidistribution can be achieved by an $\mathcal{F}$ on a particular functional form. One weight function that has been considered is the arc length of the numerical solution. Creating a mesh such that the arc length is distributed equally between the mesh points will for example ensure a clustering of mesh nodes in regions with steep gradients. Equidistribution has been shown to work well with different weight functions in FEM and FD methods [11, 12, 15], but it has not been explored much in the context of high order methods. It is usually not a suitable adaptive method in itself, since it does not ensure regularity in $\mathcal{F}$, as demonstrated in [19]. However, the same paper shows that equidistribution in conjunction with filtering can give very good results. The authors also reduce the cost of the method by solving the equidistribution problem with a low order method.

Funaro [13] proposed an adaptive collocation method where the collocation points are determined by inserting the Legendre polynomial of degree N into the given PDE. For an advection-diffusion model problem this results in a staggered mesh where the nodes are actually slightly shifted *away* from the boundary layer. Still, the numerical solution on the staggered mesh displays smaller oscillations than that obtained with the standard collocation method, and it is a better approximation of the exact solution. A favorable feature of this method is that it is applicable also in higher space dimensions, and the author shows an example by solving a boundary value problem in $\mathbb{R}^2$.

4 Constructing an optimal mapping

The adaptive high order methods mentioned so far are all constructed with the objective to adjust the mapping $\mathcal{F}$ from $\widehat{\Omega}$ to Ω in such a way that the discretization error decreases for a fixed number of degrees-of-freedom (i.e., for a fixed polynomial degree, N). A natural question to ask is then: to what extent can the mapping be used to reduce the discretization error? Let us by *optimal mapping* define the mapping $\mathcal{F}$ that, when used in the numerical solution of a given boundary value problem with a spectral method as described in Section 2, results in the smallest numerical error, measured in the L^2-norm. This particular numerical solution will be defined as the *optimal solution* of the given boundary value problem for the given method and the given polynomial degree N. Note that the optimal mapping depends on all of these factors; even changing the norm in which we measure the error may give a (slightly) different optimal $\mathcal{F}$.

The optimal $\mathcal{F}$ is not unique since information about the mapping is only required at a finite number of points. For example, using a spectral method to solve (1) with Dirichlet boundary conditions only requires the value of the Jacobian (the first derivative of $\mathcal{F}$) at the quadrature points. Any two mappings that have the same values of the derivatives at these points are not discerned by the numerical method. In the following, we will therefore assume that $\mathcal{F} \in \mathbb{P}_N(\widehat{\Omega})$ and we will denote the mapping as $\mathcal{F}_N$ to emphasize this; this corresponds to an isoparametric approach.

Finding optimal mappings adaptively is very difficult. We therefore start by considering the simpler problem of finding optimal mappings based on the exact solution. Consider an advection-diffusion problem (1) with a smooth right hand side f and homogeneous Dirichlet boundary conditions. The exact solution is a function $u(x)$ defined on Ω. As any other function it can be viewed as a *parametric curve*, using the trivial parametrization

$$\boldsymbol{u}(x) = (x, u(x)), \qquad x \in \Omega. \tag{16}$$

The curve can also be *reparametrized* by a change of variable $x = \mathcal{F}_N(\xi)$, yielding the new representation

$$\hat{\boldsymbol{u}}(\xi) = (\mathcal{F}_N(\xi), u(\mathcal{F}_N(\xi))) = (\mathcal{F}_N(\xi), \hat{u}(\xi)), \qquad \xi \in \widehat{\Omega}. \tag{17}$$

The numerical solution of the PDE, obtained with a spectral method using the (isoparametric) mapping $\mathcal{F}_N$, can be represented by

$$\hat{\boldsymbol{u}}_N(\xi) = (\mathcal{F}_N(\xi), \hat{u}_N(\xi)), \qquad \xi \in \widehat{\Omega}, \tag{18}$$

and this can be viewed as an approximation of the vector-valued function in (17).

A simple way to approximate the exact solution is through interpolation. In order to exploit the flexibility that the change of variable $\mathcal{F}_N$ offers, we consider interpolation of parametric curves. The parametric curve interpolation operator $\boldsymbol{I}_N$ is defined by applying the standard function interpolation operator I_N to each parametric function. The functions are interpolated in the (affinely mapped) GLL points. Applying the operator to (16) produces the interpolant

$$\boldsymbol{I}_N\boldsymbol{u}(x) = (I_N x, I_N u(x)) = (x, I_N u(x)), \qquad x \in \Omega, \tag{19}$$

and interpolating (17) yields

$$\boldsymbol{I}_N\hat{\boldsymbol{u}}(\xi) = (I_N\mathcal{F}_N(\xi), I_N\hat{u}(\xi)) = (\mathcal{F}_N(\xi), I_N\hat{u}(\xi)), \qquad \xi \in \widehat{\Omega}. \tag{20}$$

We will refer to these curves as *parametric interpolants*. Now, even though $\boldsymbol{u}$ and $\hat{\boldsymbol{u}}$ describe the same curve, the interpolants $\boldsymbol{I}_N\boldsymbol{u}$ and $\boldsymbol{I}_N\hat{\boldsymbol{u}}$ are generally not the same. If we let $\overline{\mathcal{F}}$ denote the affine mapping from $\widehat{\Omega}$ to Ω, and $\overline{x}_m = \overline{\mathcal{F}}(\xi_m)$, we remark that $(\overline{x}_m, u(\overline{x}_m))$ and $(\mathcal{F}_N(\xi_m), \hat{u}(\xi_m))$ are generally different points on the exact curve (unless $\mathcal{F}_N = \overline{\mathcal{F}}$).

The interpolant (19) is equivalent to classical interpolation of the function $u(x)$ in the GLL points. The interpolant (20) also corresponds to classical interpolation in the special case that $\mathcal{F}_N = \overline{\mathcal{F}}$, i.e., when $\mathcal{F}_N$ just varies linearly with ξ. However, if $\mathcal{F}_N$ is chosen wisely, then $\hat{u}$ is better suited for polynomial interpolation than u. For example, it may be a function of higher regularity, or it may have slower variation and wider boundary layers. Reparametrization can be used to "move" some of the complexity from one parametric function to the other. One can in principle consider a strongly nonlinear change of variable $x = \mathcal{F}_N(\xi)$ that yields little or no variation in $\hat{u}(\xi)$, however, this may only be possible for a very high N. A balance in complexity between the two parametric functions is most likely better in order to achieve a small interpolation error for a fixed N.

The optimal reparametrization is the one that results in minimization of the L^2-norm of the interpolation error[1]. Finding the optimal change of variable is a problem with $N+1$ free variables, since the reparametrization is uniquely determined by the value of $\mathcal{F}_N$ at the GLL points. The mapping $\mathcal{F}_N : \widehat{\Omega} \to \Omega$ such that $\mathcal{F}_N \in \mathbb{P}_N(\widehat{\Omega})$ can be represented explicitly as

$$\mathcal{F}_N(\xi) = \sum_{j=0}^{N} x_j^* \ell_j(\xi), \tag{21}$$

with $x_j^* = \mathcal{F}_N(\xi_j)$. Choosing basis coefficients x_j^* *uniquely* determines $\mathcal{F}_N$, which in turn uniquely determines the interpolant $I_N\hat{\boldsymbol{u}}$, with

$$I_N\hat{u}(\xi) = \sum_{j=0}^{N} u_j^* \ell_j(\xi), \tag{22}$$

and with $u_j^* = I_N\hat{u}(\xi_j) = u(x_j^*)$, $j = 0, \ldots, N$.

The free variables $x_0^*, \ldots, x_N^*$ represent $N+1$ *degrees-of-freedom* in the construction of the interpolant. Note how this differs from classical interpolation of functions: these degrees-of-freedom are available *after* we have chosen the GLL points as interpolation points in the reference domain. If exploited wisely, they represent a potential for parametric interpolants to be more accurate than classical interpolants.

The variables $x_0^*, \ldots, x_N^*$ can be also expressed through the affine mapping $\overline{\mathcal{F}}(\xi)$. In particular, we can write

$$x_j^* = \mathcal{F}_N(\xi_j) = \overline{\mathcal{F}}(\xi_j^*), \qquad j = 0, \ldots, N, \tag{23}$$

and thus redefine the problem of finding an optimal mapping to a problem of choosing the values $\xi_0^*, \ldots, \xi_N^*$. The choice should be restricted to values that satisfy

$$\xi_0^* < \xi_1^* < \ldots < \xi_N^*, \tag{24}$$

since $\mathcal{F}_N$ should be invertible. The monotonicity restriction (24) does not guarantee that $\mathcal{F}_N$ is invertible, since it can oscillate between the nodes, but this is a small practical problem and will not be discussed here.

[1] Since the exact curve can be represented by a single function, we measure the interpolation error between this function and the function representation of the interpolant. This is possible as long as $\mathcal{F}_N$ is invertible.

The problem of optimal choice of $\xi_0^*, \ldots, \xi_N^*$ was investigated in [7], where the *equal-tangent* (ET) method was proposed. The method reduces the number of degrees-of-freedom by two by requiring that the end points be interpolation points. This was motivated by the numerical solution of PDEs in deformed quadrilaterals in $\mathbb{R}^2$, but it also makes sense here: it ensures that the end points are nodes on the computational mesh in the physical domain, which makes imposition of the boundary conditions easy. The remaining $N-1$ free variables are determined by the condition that the interpolant also matches the tangent directions at the internal interpolation points. This can also be viewed as Hermite interpolation when considering the function representation of the curves [18]. It can be achieved by solving the system of non-linear equations

$$\frac{\mathrm{d}u}{\mathrm{d}x}(\mathcal{F}_N(\xi_j))\,\frac{\mathrm{d}\mathcal{F}_N}{\mathrm{d}\xi}(\xi_j) - \frac{\mathrm{d}I_N(u\circ\mathcal{F}_N)}{\mathrm{d}\xi}(\xi_j) = 0, \qquad j = 1, \ldots, N-1, \tag{25}$$

with respect to the $N-1$ free variables $\xi_1^*, \ldots, \xi_{N-1}^*$. The dependency of each term on the free variables is trough the coordinate transformation $\mathcal{F}_N$; see (21) and (23). We use $u \circ \mathcal{F}_N$ instead of $\hat{u}$ since we do not assume a priori knowledge of $\hat{u}$; in fact, it depends on $\mathcal{F}_N$, which in essence is the unknown here. The last term is given by

$$\frac{\mathrm{d}I_N(u\circ\mathcal{F}_N)}{\mathrm{d}\xi}(\xi) = \sum_{j=0}^{N} u(\mathcal{F}_N(\xi_j))\ell_j'(\xi). \tag{26}$$

The equations in (25) can be viewed in two ways: (i) in the reference domain they represent the difference in the derivative between of $\hat{u}$ and $I_N\hat{u}$ at the internal GLL points; (ii) in the physical domain, the equations represent the dot product between the tangent vector $(\mathcal{F}_N'(\xi_j), (I_N\hat{u})'(\xi_j))$ to the interpolant and the normal vector $(u'(\mathcal{F}_N(\xi_j)), -1)$ to the exact curve at the interpolation points. Hence, by solving the system (25) for $\xi_1^*, \ldots, \xi_{N-1}^*$, we are implicitly finding a coordinate transformation $\mathcal{F}_N$ such that the interpolant $I_N\hat{\boldsymbol{u}}$ matches both function values and derivatives of $\hat{\boldsymbol{u}}$ at the internal GLL points $\xi_1, \ldots, \xi_{N-1}$.

The system (25) is solved using Newton's method. Exact expressions for the partial derivatives of the objective function with respect to the free variables can be derived by standard techniques. In order to make the interpolation method more robust, Newton's method is run several times with different initial values, and the solution that results in the smallest interpolation error, measured in the discrete L^2-norm, is chosen. Implementation is discussed in more detail in [7].

When the ET method has produced a solution to the interpolation problem, the associated mapping $\mathcal{F}_N$ can be used in a pure spectral method for solving the given boundary value problem. Assume that the exact solution u to this problem belongs to $H^\sigma(\Omega)$ and that we construct the classical interpolant $I_N u$ associated with the GLL points. The standard interpolation error is then bounded by [6]

$$||u - I_N u||_{L^2(\Omega)} \leq cN^{-\sigma}||u||_{H^\sigma(\Omega)}, \tag{27}$$

where c is a constant. If the exact solution u is analytic ($\sigma \to \infty$), we can expect the classical interpolation error to decrease exponentially fast as the polynomial degree, N, increases. It is now of interest to consider the following two questions: (i) what difference does it make to use a non-affine mapping instead of the standard mapping? and (ii) what is the difference between the interpolation error $||u - I_N u||$ and the discretization error $||u - u_N||$ in the spectral solution of the given boundary value problem?

We illustrate these issues by revisiting the numerical example from Section 2. Figure 3 shows that a standard spectral method (i.e., using a linear mapping $\overline{\mathcal{F}}$) results in exponential convergence, but that the convergence rate can be increased dramatically by using

the ET method to construct a more appropriate mapping $\mathcal{F}_N$. Figure 3 also shows the interpolation error when interpolating the exact solution as a parametric curve, for two different parametrizations, one based on the non-affine mapping $\mathcal{F}_N$ and one based on the affine mapping $\overline{\mathcal{F}}$. As expected, the results indicate a close relationship between the discretization error and the interpolation error.

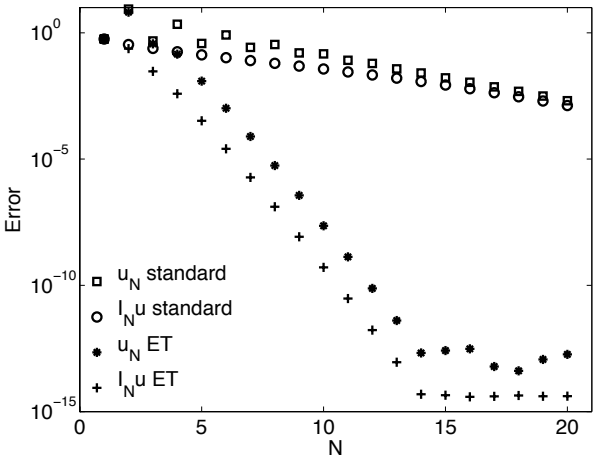

Figure 3: The error $||u-u_N||_{L^2}$ in the spectral Galerkin solution of (1) where (2) is the exact solution, and the error $||u - I_N u||_{L^2}$ in the parametric interpolation of the exact solution. The non-affine mapping $\mathcal{F}_N$ produced by the ET method gives much faster convergence than the standard (affine) mapping $\overline{\mathcal{F}}$, both when considering interpolation and numerical solution of the boundary value problem.

5 Constructing an approximate mapping

Let us now change the way we construct our non-affine mapping. In the previous section we applied the ET method to the exact solution of the original problem to construct a very good mapping $\mathcal{F}_N$. Let us now instead apply the ET method to the exact solution of a modified problem. In particular, we first change the diffusivity ε to $\tilde{\varepsilon}$ (with $\tilde{\varepsilon} \geq \varepsilon$) in the advection-diffusion problem (1). The exact solution of this modified problem has a thicker boundary layer compared to the original problem. We now apply the ET method to the exact solution of the modified problem and construct a corresponding non-affine mapping $\mathcal{F}_N(\xi;\tilde{\varepsilon})$ (the argument is added to remind us that the mapping constructed this way depends on the diffusivity $\tilde{\varepsilon}$ chosen in the approximate problem). Finally, we use the mapping $\mathcal{F}_N(\xi;\tilde{\varepsilon})$ in the spectral Galerkin solution of the original problem. In Figure 4 we show the discretization error as a function of the polynomial degree, N, for $\tilde{\varepsilon} = 0.1$, $\tilde{\varepsilon} = 0.02$ and $\tilde{\varepsilon} = \varepsilon = 0.01$ (i.e., corresponding to the results of the previous section). We notice that significant improvement from using the standard affine mapping is achieved. However, the results also show a high degree of sensitivity to the quality of the mapping used.

6 Adaptivity through minimization of the residual

6.1 Residual of the strong form

If we want to construct an adaptive method to find the optimal solution of a given boundary value problem, we immediately face a problem: our definition of the optimal solution as

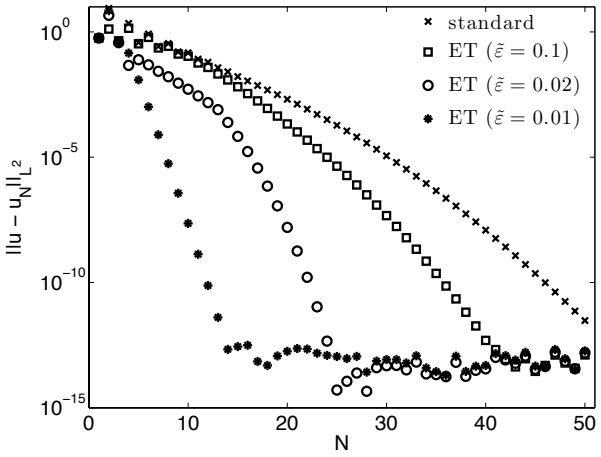

Figure 4: The error $||u - u_N||_{L^2}$ in the spectral Galerkin solution of (1) where (2) is the exact solution. The non-affine mapping $\mathcal{F}_N(\xi; \tilde{\varepsilon})$ used here is constructed by applying the ET method to the exact solution of a modified advection-diffusion problem with a diffusivity $\tilde{\varepsilon} \geq \varepsilon$.

the L^2-minimizer of the error in the numerical solution of the PDE does not lend itself to adaptivity, since the evaluation of the error involves the exact solution; an adaptive method cannot assume any knowledge of the exact solution.

The most valuable information we have about the approximation properties of a numerical solution of a boundary value problem is the residual. It may give information about about the magnitude of the numerical error, as well as the location of the areas where the numerical solution represents a poor (or good) approximation of the exact solution. An adaptive method can in principle be constructed by minimizing the residual.

Consider an advection-diffusion problem on the form (1) with Dirichlet boundary conditions, and assume that we apply a spectral method as shown in Section 2, using a polynomial mapping $\mathcal{F}_N$. The residual of the strong form is then given by

$$r_N(x) = f(x) - f_N(x), \tag{28}$$

where $f(x)$ is the right hand side of the PDE and

$$f_N(x) = -\varepsilon \frac{\mathrm{d}^2 u_N}{\mathrm{d}x^2} + \frac{\mathrm{d}u_N}{\mathrm{d}x} \tag{29}$$

is the numerical solution (2) inserted into the left hand side of the PDE.

Figure 5 shows some examples of the residual (28) when solving the model problem from Section 2. In the particular case of using a standard spectral Galerkin method (including an affine mapping), all the integrals in the weak form are computed without any quadrature error using standard GLL quadrature, including the right hand side since f is only a constant. The numerical solution is therefore also a solution of the strong form of the problem, and hence the residual is zero at the mesh nodes. This is not the case for the ET solution, which gives zero residual at other points throughout the domain. The standard method gives poor approximation and large residual in the entire domain for small N, whereas the ET method has managed a good approximation of the outer solution even for relatively small N. The residual is relatively large in the boundary layer, but here it decreases very rapidly as N increases.

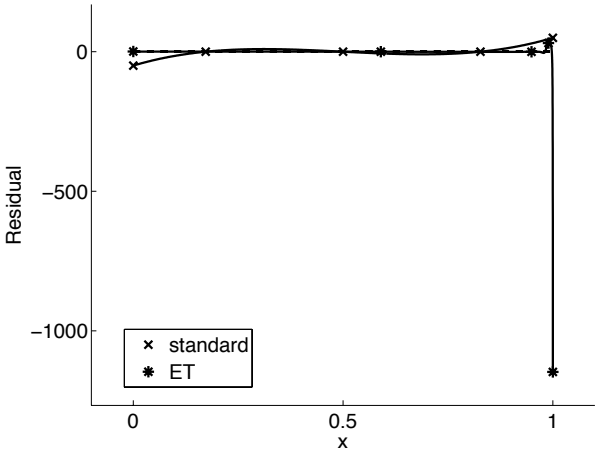

(a) $N = 4$

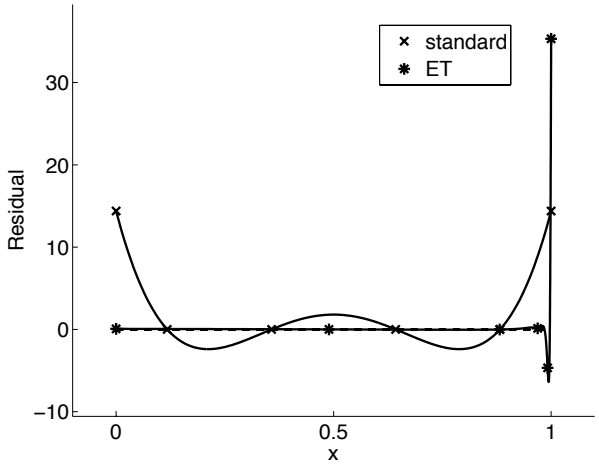

(b) $N = 5$

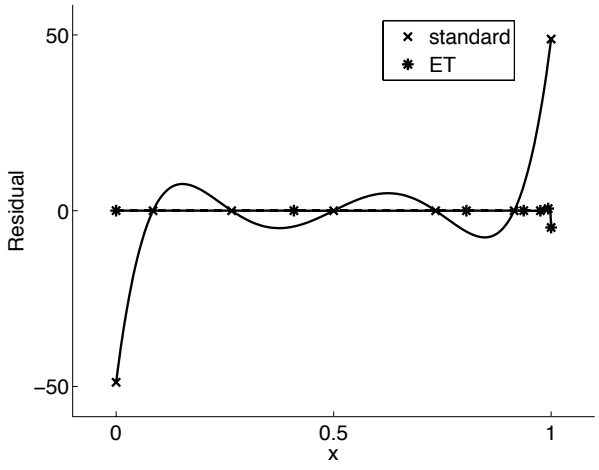

(c) $N = 6$

Figure 5: The residual (28) of the strong form after computing the spectral Galerkin solution of the advection-diffusion problem (1) with exact solution (2). The standard method (i.e., using an affine mapping) results in a large residual over the entire domain, whereas a non-affine mapping produced by the ET method confines the inaccuracy to a very thin boundary layer.

In the following, we will only consider the strong form of the residual when discussing potential ways to construct adaptive spectral methods. This choice has been made in order to simplify as much as possible the implementation and assessment of such an approach.

6.2 Unconstrained minimization of the residual

A measure of the quality of the numerical solution of the boundary value problem can be given by the residual of the strong form measured in the L^2-norm,

$$||f - f_N||^2_{L^2(\Omega)} = \int_\Omega r_N(x)^2 \, \mathrm{d}x, \tag{30}$$

which is most conveniently evaluated over the reference domain. Mapping the residual to the reference domain yields

$$\hat{r}_N(\xi) = \hat{f}(\xi) - \hat{f}_N(\xi), \tag{31}$$

where $\hat{f}(\xi) = f(\mathcal{F}_N(\xi))$ and

$$\hat{f}_N(\xi) = -\varepsilon \frac{\hat{u}''_N(\xi)\mathcal{F}'_N(\xi) - \mathcal{F}''_N(\xi)\hat{u}'_N(\xi)}{(\mathcal{F}'_N(\xi))^3} + \frac{\hat{u}'_N(\xi)}{\mathcal{F}'_N(\xi)} \tag{32}$$

Applying quadrature with over-integration in $M \gg N$ points to ensure subdominant quadrature error yields the discrete norm

$$||f - f_N||_N = \Big(\sum_{\alpha=0}^{M} \rho_\alpha \hat{r}_N(\xi_\alpha)^2 \mathcal{F}'_N(\xi_\alpha) \Big)^{1/2}. \tag{33}$$

An adaptive method can now in principle be defined by minimizing the functional

$$\mathcal{J} = ||f - f_N||^2_N. \tag{34}$$

At this point, both $\mathcal{F}_N$ and $\hat{u}_N$ are unknown. Similar to the case of interpolating the exact solution (see Section 4), the mapping $\mathcal{F}_N$ is given by (21) and (23). The numerical solution $\hat{u}_N$ is also expressed through a nodal basis similar to (22). The simplest implementation of the minimization procedure is achieved when letting both $\xi^*_1, \ldots, \xi^*_{N-1}$ and the basis coefficients $u^*_1, \ldots, u^*_{N-1}$ be free variables. This means that we do not solve (1) numerically at this point, but rather let the minimizer of $\mathcal{J}$ define the mapping $\mathcal{F}_N$ that is subsequently used in a spectral method to compute $\hat{u}_N$. However, we keep a link with the boundary value problem by letting $\xi^*_0, \xi^*_N, u^*_0, u^*_N$ be determined by the boundary conditions.

The minimum of $\mathcal{J}$ occurs at a stationary point, which is a solution of the system

$$\begin{aligned} \frac{\partial \mathcal{J}}{\partial \xi^*_i} &= 0, \qquad i = 1, \ldots, N-1, \\ \frac{\partial \mathcal{J}}{\partial u^*_i} &= 0, \qquad i = 1, \ldots, N-1. \end{aligned} \tag{35}$$

Of course, $\mathcal{J}$ may have several stationary points, corresponding to different *local* minima (and maxima). A crude *global* minimization procedure is constructed by solving (35) several times, using Newton's method, but with different initial values. The solution that gives the smallest value of $\mathcal{J}$ is then chosen. As the polynomial degree N increases, an exhaustive search for the global minimizer will be infeasible (as the number of free variables becomes too large), but with good initial values this minimization method may be sufficient to find close to optimal solutions.

The result of the minimization procedure is set of variables that define $\mathcal{F}_N$ and $\hat{u}_N$. We discard $\hat{u}_N$ and use a spectral method based on $\mathcal{F}_N$ to solve (1) numerically. This completes the adaptive method, which we will refer to as the *unconstrained minimum residual* (UMR) method.

Let us write out the terms in (35). The partial derivative of $\mathcal{J}$ with respect to ξ_i^* is

$$\frac{\partial \mathcal{J}}{\partial \xi_i^*} = \sum_{\alpha=0}^{M} \rho_\alpha \left(2\, \hat{r}_N(\xi_\alpha)\, \frac{\partial \hat{r}_N}{\partial \xi_i^*}(\xi_\alpha) \mathcal{F}_N'(\xi_\alpha) + \hat{r}_N(\xi_\alpha)^2\, \frac{\partial \mathcal{F}_N'}{\partial \xi_i^*}(\xi_\alpha) \right), \tag{36}$$

where prime means derivative with respect to the free variable ξ on $\widehat{\Omega}$. The partial derivative of the residual is

$$\begin{aligned} \frac{\partial \hat{r}_N}{\partial \xi_i^*} =& f'(\mathcal{F}_N(\xi)) \frac{\partial \mathcal{F}_N}{\partial \xi_i^*} + \hat{u}_N'(\xi) \mathcal{F}_N'(\xi)^{-2} \frac{\partial \mathcal{F}_N'}{\partial \xi_i^*} \\ &+ \varepsilon \mathcal{F}_N'(\xi)^{-4} \left(3\hat{u}_N'(\xi) \mathcal{F}_N''(\xi) \frac{\partial \mathcal{F}_N'}{\partial \xi_i^*} - \hat{u}_N'(\xi) \mathcal{F}_N'(\xi) \frac{\partial \mathcal{F}_N''}{\partial \xi_i^*} - 2\hat{u}_N''(\xi) \mathcal{F}_N'(\xi) \frac{\partial \mathcal{F}_N'}{\partial \xi_i^*} \right). \end{aligned} \tag{37}$$

Note that $\hat{u}_N$ and its derivatives do not depend on ξ_i^* since $\hat{u}_N$ is not a numerical solution of the boundary value problem at this point; it is one of the unknowns. From the representation (21) of $\mathcal{F}_N$ we see that

$$\frac{\partial \mathcal{F}_N}{\partial \xi_i^*} = c\, \ell_i(\xi), \qquad \frac{\partial \mathcal{F}_N'}{\partial \xi_i^*} = c\, \ell_i'(\xi) \qquad \text{and} \qquad \frac{\partial \mathcal{F}_N''}{\partial \xi_i^*} = c\, \ell_i''(\xi), \tag{38}$$

where $c = \overline{\mathcal{F}}'(\xi)$ is a constant. The partial derivative of $\mathcal{J}$ with respect to u_i^* is simply

$$\frac{\partial \mathcal{J}}{\partial u_i^*} = 2 \sum_{\alpha=0}^{M} \rho_\alpha \hat{r}_N(\xi_\alpha) \frac{\partial \hat{r}_N}{\partial u_i^*}(\xi_\alpha) \mathcal{F}_N'(\xi_\alpha), \tag{39}$$

since $\mathcal{F}_N$ does not depend on any of the u_i^*. The partial derivative of the residual is

$$\frac{\partial \hat{r}_N}{\partial u_i^*} = -\frac{\varepsilon}{\mathcal{F}_N'(\xi)^2} \frac{\partial \hat{u}_N''}{\partial u_i^*} + \left(\frac{\varepsilon \mathcal{F}_N''(\xi)}{\mathcal{F}_N'(\xi)^3} + \frac{1}{\mathcal{F}_N'(\xi)} \right) \frac{\partial \hat{u}_N'}{\partial u_i^*}, \tag{40}$$

where

$$\frac{\partial \hat{u}_N'}{\partial u_i^*} = \ell_i'(\xi) \qquad \text{and} \qquad \frac{\partial \hat{u}_N''}{\partial u_i^*} = \ell_i''(\xi). \tag{41}$$

The expressions above are needed just to evaluate (35). Newton's method additionally requires the partial derivatives of each equation in (35) with respect to each free variable. The resulting $2(N-1) \times 2(N-1)$ Hessian matrix is quite complicated, but can be found explicitly through repeated partial differentiation.

We apply the UMR method in the numerical solution of the advection-diffusion problem (1) with $f = 1$ and exact solution (2). Figure 6 shows that the UMR method almost keeps up with the ET method (as discussed in Section 4) for small N, but that the convergence rate decreases as N increases. This is most likely due to the difficulty of solving the global minimization problem.

6.3 Constrained minimization of the residual

One possible way to improve the UMR method is to solve the boundary value problem in conjunction with the minimization problem. In the UMR method, the minimization

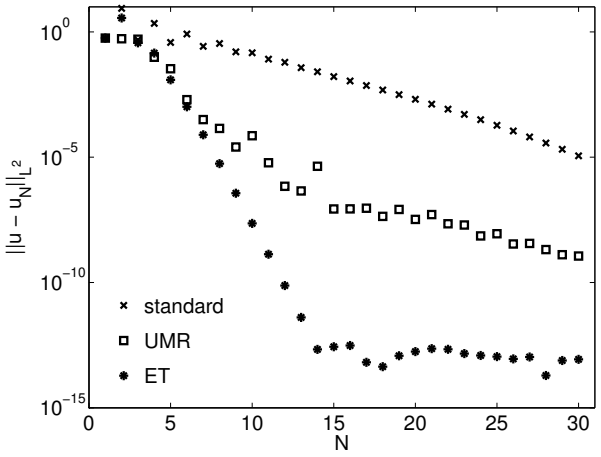

Figure 6: The error in the numerical solution of the advection-diffusion problem (1) with exact solution (2). The UMR method gives an improvement compared to a standard spectral method (i.e., using an affine mapping), and it keeps up with the solution obtained by the ET-method (as discussed in Section 4) for low values of N. However, as N increases the convergence rate decreases due to the complexity of the system of nonlinear equations that must be solved.

procedure does not take into account which numerical method is used to ultimately solve the boundary value problem. The minimization procedure would be the same if we switched from a spectral method to a PS method or another method.

Solving the minimization problem and the boundary value problem simultaneously means minimizing $\mathcal{J}$ subject to the *constraint* that $\hat{u}_N$ is a numerical solution of (1). The resulting adaptive method will be referred to as the *minimum residual* (MR) method, and it is most conveniently implemented by considering a PS method for the numerical solution of the boundary value problem. This means that the constraints are $\hat{r}_N(\xi_j) = 0$, $j = 1, \ldots, N-1$, i.e., vanishing residual (of the strong form) in the internal GLL points. The constrained minimization problem can be solved by considering the Lagrange function

$$\Lambda = \mathcal{J} + \sum_{k=1}^{N-1} \lambda_k \hat{r}_N(\xi_k), \tag{42}$$

where λ_k are the Lagrange multipliers. Solutions of the constrained minimization problem are stationary points for Λ, which is a function of $\xi_1^*, \ldots, \xi_{N-1}^*$, $u_1^*, \ldots, u_{N-1}^*$ and $\lambda_1, \ldots, \lambda_{N-1}$. Finding a stationary point means solving a system of $3(N-1)$ nonlinear equations,

$$\begin{aligned}
\frac{\partial \Lambda}{\partial \xi_i^*} &= \frac{\partial \mathcal{J}}{\partial \xi_i^*} + \sum_{k=1}^{N-1} \lambda_k \frac{\partial \hat{r}_N}{\partial \xi_i^*}(\xi_k) &&= 0, \qquad i = 1, \ldots, N-1, \\
\frac{\partial \Lambda}{\partial u_i^*} &= \frac{\partial \mathcal{J}}{\partial u_i^*} + \sum_{k=1}^{N-1} \lambda_k \frac{\partial \hat{r}_N}{\partial u_i^*}(\xi_k) &&= 0, \qquad i = 1, \ldots, N-1, \\
\frac{\partial \Lambda}{\partial \lambda_i} &= \hat{r}_N(\xi_i) &&= 0, \qquad i = 1, \ldots, N-1.
\end{aligned} \tag{43}$$

Note that even if this system is larger than (35), it is not much more complicated. The partial derivatives of $\mathcal{J}$ are the same as (36) and (39), and due to our choice of using a PS method we can reuse the partial derivatives (37) and (40) of $\hat{r}_N$.

In order to find solutions of (43) we again employ Newton's method. The implementation is basically the same as for the UMR method.

The MR method should, by construction, give the optimal solution in terms of the residual, which again is very close to the optimal solution as defined in Section 4. However, this requires us to find the best of all possible solutions to (43). Figure 7 shows that we get the same convergence rate as the ET method for low values of N; this is an indication that the solution may be close to optimal. However, the convergence rate decreases as N increases, just as in Figure 6, most likely for the same reason.

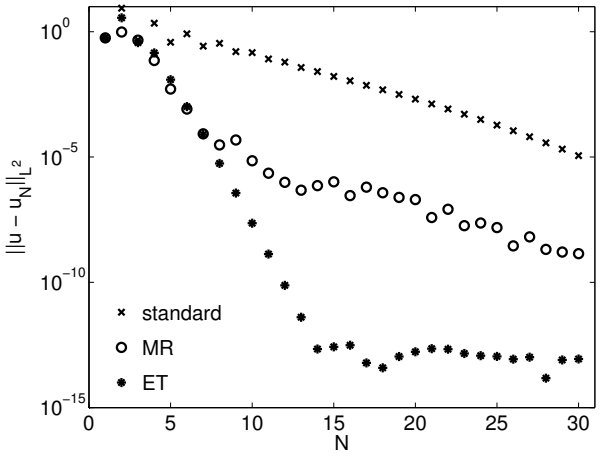

Figure 7: The error in the numerical solution of the advection-diffusion problem (1) with exact solution (2). The MR method almost keeps up with the ET method (as discussed in Section 4) for small values of N, but the convergence rate decreases as N increases since the minimization problem becomes more difficult to solve.

7 Adaptivity through residual-based interpolation

The excellent results achieved with the ET method applied to the exact solution in Section 4 motivates an investigation of how it may be used in an adaptive method, but now without using any information about the exact solution. We first recall that the ET method is based on using the available degrees-of-freedom to ensure that the error in the derivative is zero at the internal interpolation points. In the context of solving PDEs, the collocation method gives zero residual at the grid points, but has typically nonzero derivatives at these points, e.g., see the results in Figure 5 for the standard method. A parallel to the ET method would be to use the available degrees-of-freedom to also make the derivative of the residual zero at the internal grid points. This means finding a mapping $\mathcal{F}_N(\xi)$ such that

$$\hat{r}'_N(\xi_j) = \hat{f}'(\xi_j) - \hat{f}'_N(\xi_j) = 0, \qquad j = 1, \ldots, N-1. \tag{44}$$

To make sure that zero residual is also satisfied, we must solve these equations together with the collocation equations

$$\hat{r}_N(\xi_j) = \hat{f}(\xi_j) - \hat{f}_N(\xi_j) = 0, \qquad j = 1, \ldots, N-1. \tag{45}$$

As before, we use Newton's method for the solution of the coupled system of nonlinear equations. The Jacobian matrix of the system can be derived using (37) and (40) and normal differentiation rules. Since the system may have more than one solution, we repeat

our strategy of solving the system several times with different initial values, and choose the solution with the smallest L^2-error. We will refer to this method as the *equal-tangent residual* (ETR) method.

Figure 8 shows a convergence plot for the same test problem as before. There is some improvement from the standard method, but the new method is not able to find the optimal solution.

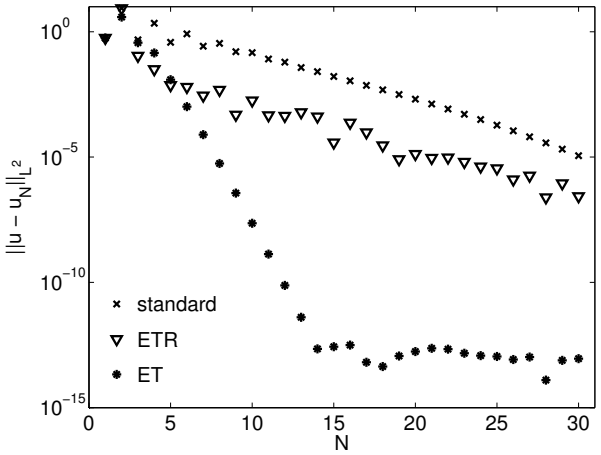

Figure 8: The error in the numerical solution of the model problem (1) with exact solution (2). The ETR method gives a certain improvement from the standard method, but does not match the convergence rate of the ET method.

8 Additional numerical results

Let us now consider a few more numerical examples in order to compare the various methods proposed earlier. Again, we consider the advection-diffusion boundary value problem (1) with $\varepsilon = 0.01$, but now for different choices of f.

Figure 9 shows a convergence plot when the exact solution is given as

$$u(x) = \frac{1}{2}\big(1 - \frac{\operatorname{erf}(x/\sqrt{\varepsilon})}{\operatorname{erf}(1/\sqrt{\varepsilon})}\big), \qquad x \in [-1, 1]. \tag{46}$$

This solution has an interior layer of width $\mathcal{O}(\varepsilon)$ around $x = 0$. The ETR and the UMR method only keep up with the ET method for very low N; the error then decreases very slowly as N increases. The MR method gives better results, since it is able to follow the ET convergence rate a little longer.

When the exact solution is given as

$$u(x) = \frac{1}{2}(1 - x)(\arctan(\frac{1 + x}{(2 - a)\varepsilon}) + \arctan(\frac{a}{\varepsilon})), \qquad x \in [-1, 1], \tag{47}$$

where $a = 0.35$, we get an interior layer of width $\mathcal{O}(\varepsilon)$ near $x = 2a - 1 = -0.3$. Figure 10 shows that the UMR method is not very successful in this case, although it suddenly finds a better solution after $N = 20$. This may be caused by a lucky choice of initial value for the Newton iterations. The ETR method, on the other hand, gives markedly better performance, and the MR method gives an even better convergence rate.

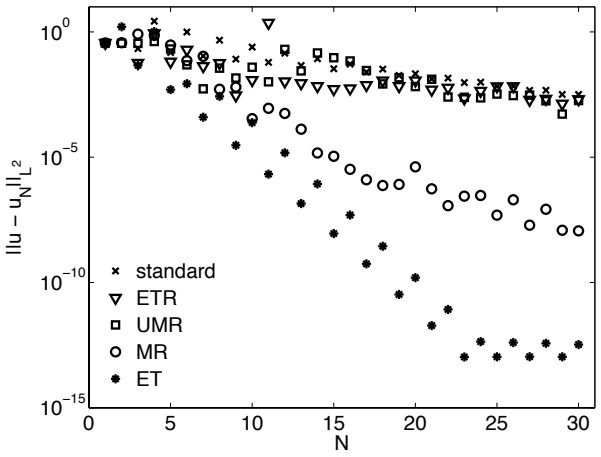

Figure 9: The error in the numerical solution of the advection-diffusion problem (1) with exact solution (46), which has an interior layer near $x = 0$. Of the adaptive methods, only the MR method gives a clear improvement from the standard method.

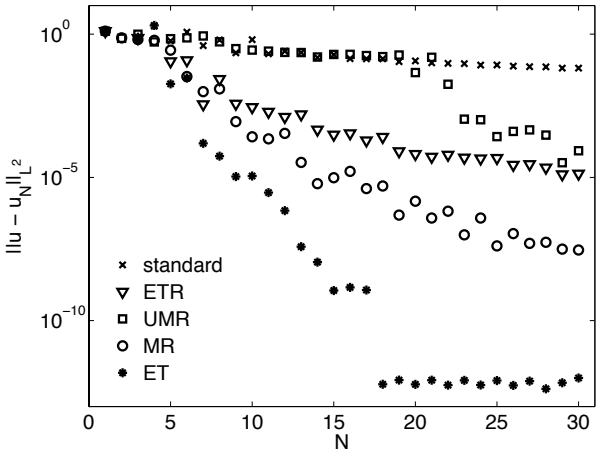

Figure 10: The error in the numerical solution of the advection-diffusion problem (1) with exact solution (47), which has an interior layer near $x = -0.3$. Again the adaptive methods lose track of the ET convergence rate very early, but they maintain a good convergence rate as N increases, making them far more accurate than the standard method.

9 Conclusions

We have proposed several methods for constructing coordinate transformations for spectral and PS methods, and these have sometimes yielded significant improvement compared to standard methods. Improvement here means smaller discretization error for a fixed polynomial degree, N, used in the approximation.

The methods that are based on a direct minimization of the residual of the strong form should, by construction, give close to optimal solutions. However, these methods require proper global minimization procedures, something which is very difficult and computationally expensive to achieve. The minimization method used in this work sometimes yields close to optimal convergence rate for low N, but the convergence rate often decreases as N increases; this is primarily due to the increasing difficulty of solving the global minimization problem. One conclusion from this effort is therefore that it is difficult to construct efficient and robust adaptive methods based on minimization of the residual since good

global minimization procedures are often computationally expensive, and the added cost typically outweigh the increased accuracy for a given N.

We have also proposed a way to construct close to optimal nonlinear mappings for spectral and PS methods based on information about the exact solution. The approach uses the equal-tangent (ET) method investigated in [7] to first construct an interpolant of the exact solution, viewed as a parametric curve, and then employs this interpolant to define the mapping used in a subsequent spectral Galerkin method to solve the given boundary value problem. The method does not qualify as an adaptive method since it requires knowledge of the exact solution, but it is useful for providing benchmark solutions to model problems.

An adaptive method based on the same idea as the ET method has also been proposed; this method is based on requiring zero derivative of the residual of the strong form in the nodal points of the solution. The method often gives an improvement from the standard spectral method, but the convergence rate is rarely optimal.

The methods proposed and tested in this paper are relatively expensive computationally. A cost-benefit test has not been performed, since efficiency has not been the main focus of this work. The problem of finding optimal adaptive solutions of even the simplest boundary value problems is so hard that even brute-force solutions do not always succeed. Hence, just finding solutions has taken precedence over efficiency in this preliminary study. A lot of work remains to be done in order to find efficient and robust adaptive methods for the numerical solutions of PDEs using spectral methods.

Acknowledgment

The authors would like to thank Professor Yvon Maday of Paris VI for many helpful comments and suggestions. This work has been supported by the Research Council of Norway under contract 185336/V30. The support is gratefully acknowledged.

References

[1] J. Augenbaum. An adaptive pseudospectral method for discontinuous problems. *Applied Numerical Mathematics*, 5(6):459–480, 1989.

[2] I. Babuška and W. C. Rheinboldt. Analysis of optimal finite-element meshes in $\mathbf{R}^1$. *Math. Comp.*, 33(146):435–463, 1979.

[3] R. Baltensperger, J.-P. Berrut, and B. Noël. Exponential convergence of a linear rational interpolant between transformed Chebyshev points. *Math. Comp.*, 68(227):1109–1120, 1999.

[4] A. Bayliss, D. Gottlieb, B. Matkowsky, and M. Minkoff. An adaptive pseudo-spectral method for reaction diffusion problems. *J. Comput. Phys.*, 81(2):421–443, 1989.

[5] A. Bayliss and B. Matkowsky. Fronts, relaxation oscillations, and period doubling in solid fuel combustion. *J. Comput. Phys.*, 71(1):147–168, 1987.

[6] C. Bernardi and Y. Maday. *Spectral methods*, pages 209–485. Handbook of Numerical Analysis. Volume V: Techniques of Scientific Computing (Part 2), edited by P.G. Ciarlet and J.L. Lions. Elsevier, 1997.

[7] T. Bjøntegaard, E. M. Rønquist, and Ø. Tråsdahl. Spectral approximation of partial differential equations in highly distorted domains. *J. Sci. Comput.*, in press. DOI: 10.1007/s10915-011-9561-8.

[8] F. Brezzi, M. O. Bristeau, L. P. Franca, M. Mallet, and G. Rogé. A relationship between stabilized finite element methods and the Galerkin method with bubble functions. *Comput. Methods Appl. Mech. Engrg.*, 96(1):117–129, 1992.

[9] C. Canuto. Stabilization of spectral methods by finite element bubble functions. *Comput. Methods Appl. Mech. Engrg.*, 116(1-4):13–26, 1994. ICOSAHOM'92 (Montpellier, 1992).

[10] C. Canuto, M. Y. Hussaini, A. Quarteroni, and T. A. Zang. *Spectral Methods, Fundamentals in Single Domains*. Springer, 2006.

[11] G. F. Carey and H. T. Dinh. Grading functions and mesh redistribution. *SIAM J. Numer. Anal.*, 22(5):1028–1040, 1985.

[12] T.-F. Chen, G. J. Fix, and H. D. Yang. Numerical studies of optimal grid construction. *Numer. Methods Partial Differential Equations*, 12(2):191–206, 1996.

[13] D. Funaro. A new scheme for the approximation of advection-diffusion equations by collocation. *SIAM J. Numer. Anal.*, 30(6):1664–1676, 1993.

[14] N. Hale and T. W. Tee. Conformal maps to multiply slit domains and applications. *SIAM J. Sci. Comput.*, 31(4):3195–3215, 2009.

[15] W. Z. Huang and D. M. Sloan. A simple adaptive grid method in two dimensions. *SIAM J. Sci. Comput.*, 15(4):776–797, 1994.

[16] D. Kosloff and H. Tal-Ezer. A modified Chebyshev pseudospectral method with an $O(N^{-1})$ time step restriction. *J. Comput. Phys.*, 104(2):457–469, 1993.

[17] W. B. Liu and J. Shen. A new efficient spectral Galerkin method for singular perturbation problems. *J. Sci. Comput.*, 11(4):411–437, 1996.

[18] K. Mørken. On geometric interpolation of parametric surfaces. *Computer Aided Geometric Design*, 22(9):838–848, 2005.

[19] L. S. Mulholland, W.-Z. Huang, and D. M. Sloan. Pseudospectral solution of near-singular problems using numerical coordinate transformations based on adaptivity. *SIAM J. Sci. Comput.*, 19(4):1261–1289, 1998.

[20] F. Pasquarelli and A. Quarteroni. Effective spectral approximations of convection-diffusion equations. *Comput. Methods Appl. Mech. Engrg.*, 116(1-4):39–51, 1994. ICOSAHOM'92 (Montpellier, 1992).

[21] J. Shen and L.-L. Wang. Error analysis for mapped Legendre spectral and pseudospectral methods. *SIAM J. Numer. Anal.*, 42(1):326–349, 2004.

[22] E. Tadmor. Convergence of spectral methods for nonlinear conservation laws. *SIAM J. Numer. Anal.*, 26(1):30–44, 1989.

[23] E. Tadmor. Shock capturing by the spectral viscosity method. *Comput. Methods Appl. Mech. Engrg.*, 80(1-3):197–208, 1990.

[24] T. Tang and M. R. Trummer. Boundary layer resolving pseudospectral methods for singular perturbation problems. *SIAM J. Sci. Comput.*, 17(2):430–438, 1996.

[25] T. W. Tee and L. N. Trefethen. A rational spectral collocation method with adaptively transformed Chebyshev grid points. *SIAM J. Sci. Comput.*, 28(5):1798–1811, 2006.

[26] R. Verfürth. *A Review of A Posteriori Error Estimation and Adaptive Mesh Refinement Techniques*. John Wiley, 1996.

[27] L.-L. Wang and J. Shen. Error analysis for mapped Jacobi spectral methods. *J. Sci. Comput.*, 24(2):183–218, 2005.